Angular Distributions and Total Cross Sections of Charged Particles from Li^6+Li^6 as a Function of Energy*

K. G. KIBLER†
Department of Physics and Astronomy, University of Iowa, Iowa City, Iowa
(Received 27 June 1966; revised manuscript received 28 July 1966)

The Li^6+Li^6 reaction has been studied at 13 incident energies between 2.4 and 9.0 MeV, using a dE/dx-E particle identification system and an on-line computer. Total cross sections and angular distributions were obtained for protons from the first 12 levels of B^{11}, deuterons from the first 5 $T=0$ levels in B^{10}, and tritons from the B^9 ground state. Noticeable variations in the proton angular distributions as a function of bombarding energy and indications of a $(2J+1)$ dependence of the proton cross sections as the bombarding energy was increased are indicative of compound nucleus effects. On the other hand, in the deuteron results, the dominant reaction mechanism is the transfer of an alpha particle. This process is favored for the residual states which are formed by $l_\alpha=0$ transfer. There is no evidence for strong structure in the yield curves for the deuteron groups from one energy to the next. Simple considerations of the transfer as a tunneling process, possibly modified by the presence of a long-range effective interaction, adequately describe the deuteron cross sections. Measurements were made on the ground-state deuteron group at a bombarding energy corresponding to measurements on the inverse reaction, $B^{10}(d,Li^6)Li^6$, and the angular distribution and total cross section are in good agreement. The differential cross-section ratio of the 16.62- to 16.92-MeV levels in the $Li^6(Li^6,\alpha)Be^8$ reaction was also measured and found to be 1.20 ± 0.10 and constant as a function of Li^6 energy.

INTRODUCTION

REACTIONS between complex nuclei have been studied both theoretically and experimentally with increasing vigor in the past few years. A recent review by Greider[1] summarizes the more successful attempts to describe these reactions. At incident energies well below and well above the Coulomb barrier, the experimental data may often be explained by using fairly simple models. Below the barrier, one often takes the Coulomb potential to be the dominant interaction, and semiclassical descriptions are often quite good. Far above the barrier, the effects of nuclear absorption may be most important, and in this region diffraction models have been successful to a large extent.

Multinucleon transfer reactions, such as (Li^6,α) and (Li^6,d) in the present case, should often be quite useful in selectively populating residual states. Extensive work on two-nucleon transfer (cf. Ref. 2) has been done,[2] and some success has been achieved in deuteron-transfer reactions.[3] Direct-reaction analysis of α transfer using the distorted-wave Born approximation (DWBA) has been moderately successful in some (d,Li^6) reactions.[4] In this experiment, the residual Be^8 populated by (Li^6,α) presents a somewhat different problem, but the angular distributions for (Li^6,d) should be quite interesting in the light of the inverse-reaction work.[5]

Li-induced reactions have been frequently studied, and the more extensive attempts at a systematic examination of these reactions have been the work of Huberman *et al.*[6] at Chicago, and Heikkinen[7] and McGrath[8] at Iowa. The Chicago work at 2.1 MeV was well below the barrier, and the results strongly suggested that a favored reaction mechanism was via clusters, of which $Li^6(\alpha+d)$ and $Li^7(\alpha+t)$ may be taken to consist. The quite recent work of Heikkinen[7] and McGrath[8] (both experiments at higher energy, but still below the Coulomb barrier in the incident channel) suggest that both compound-nucleus and direct modes are important. In the latter work, a noticeable $2J+1$ dependence of the cross section was taken to infer that a statistical compound-nucleus picture was applicable, particularly for low-lying levels of the residual nuclei.

In the present experiment the Li^6+Li^6 reaction has been studied at 13 incident energies between 2.4 and 9.0 MeV. The two highest energy runs at 9.0 and 7.35 MeV were taken during the initial testing period of our carbon-foil stripper. This energy range extends from the region well below the Coulomb barrier (4.8 MeV in the lab) to well above the barrier, so a useful comparison with several of the simple phenomenological models for complex-nucleus reactions may be obtained. This work nearly joins the extensive work of Chicago[6] at the low-energy end, extends through the complicated Coulomb-barrier region (eight energies were investigated between 4.0 and 5.5 MeV), and overlaps the work of Gemmell *et al.*[5] on the inverse reaction $B^{10}(d,Li^6)Li^6$ done at Argonne. In fact, the run done at 7.35 MeV corresponds to the same center-of-mass energy as the 8.0-MeV Argonne data, which provides a useful comparison of results from inverse reactions.

The residual nuclei populated are not particularly simple to interpret theoretically, since they are in the

* Research supported in part by the National Science Foundation.
† Work performed while United States Steel Foundation Postgraduate Fellow 1965–1966.
[1] K. Greider, Ann. Rev. Nucl. Sci. **15**, 291 (1965).
[2] N. K. Glendenning, Ann. Rev. Nucl. Sci. **13**, 191 (1963).
[3] D. A. Bromley, Argonne National Laboratory Report No. 6878, Vol. II, p. 353 (unpublished).
[4] W. W. Daehnick and L. J. Denes, Phys. Rev. **136**, B1325 (1964).
[5] D. S. Gemmell, J. R. Erskine, and J. P. Schiffer, Phys. Rev. **134**, B110 (1964).
[6] M. N. Huberman, M. Kamegai, and G. C. Morrison, Phys. Rev. **129**, 791 (1963).
[7] D. W. Heikkinen, Phys. Rev. **141**, 1007 (1966).
[8] R. L. McGrath, Phys. Rev. **145**, 802 (1966).

middle of the $1p$ shell. This region represents a position between the extremes of LS- and jj-coupling limits, but has been described with reasonable success in the intermediate-coupling[9] and unified-model[10] pictures. The (Li^6,p) reaction here populates levels in B^{11}, of which the following were observed in the present experiment (energies in MeV): 0.0, 2.14, 4.46, 5.03, 6.76–6.81 (unresolved), 7.30, 7.99, 8.57, 8.92, 9.19–9.28 (unresolved). These levels are explained quite well in most cases by Kurath,[9] and the electromagnetic transitions between them were reported in an extensive recent paper.[11] The (Li^6,d) reaction results in the following B^{10} levels here observed: 0.0, 0.717, 2.15, 3.59, 4.77 MeV. The two highest levels were, in general, observable only at the two highest incident energies. The 1.74-MeV state was not observed, in agreement with previous work.[12] The (Li^6,t) reaction results in only one observable state here, the ground state, because of the low Q value (0.81 MeV). In addition, the ground state in B^9 is unbound to proton emission by nearly 200 keV, which probably results in a continuum from three-body effects. The α particles from the (Li^6,α) reaction have been extensively considered by several laboratories, particularly the low excitation region. Because of the low Q values in the present experiment for deuterons and tritons, amplifier gains and experimental conditions were set to maximize detail in the lower energy region. With this configuration, the highest energy α's were cutoff at all but back angles. Attention was therefore given to the high excitation region in Be^8, particularly the 16-MeV states, which have received much attention recently from Marion,[13] for example. Figure 1 summarizes the energy systematics for the residual nuclei with which we are concerned.

Thus this reaction should be quite useful not only from the viewpoint of having been studied over an energy range in which several models may be applicable, but also because final states are populated in nuclei with quite different character.

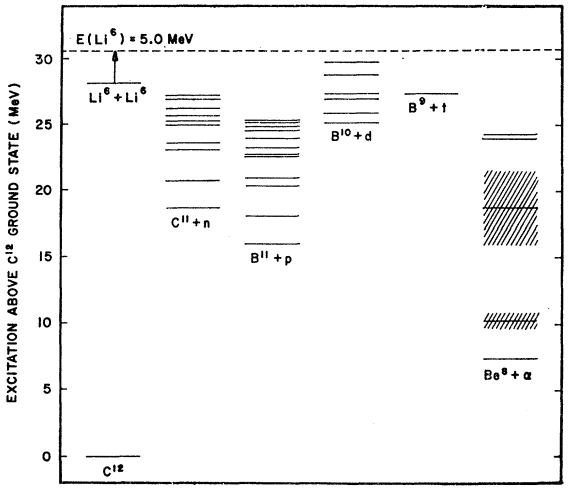

FIG. 1. Energy systematics for the Li^6+Li^6 reaction. The ordinate gives the excitation in MeV above the C^{12} ground state.

EXPERIMENTAL PROCEDURE

The Li^6 beam was produced by the University of Iowa 5.5-MeV Van de Graaff and momentum-analyzed by a 90° magnet. From the $Li^7(p,n)Be^7$ reaction, the absolute energy calibration of the accelerator is known to $\pm 0.2\%$.

As mentioned in the Introduction, the two highest energy runs were taken during the initial testing of a carbon-foil stripping section. The accelerator tube of the CN Van de Graaff normally is in two sections, and the region between these tube sections was equipped with a drift tube at the time of the initial machine installation. In this field-free region, a stripping cell was inserted. This is located at a position equivalent to 42% of the total voltage drop from the terminal. It basically consists of a rotating wheel physically shielded above and below, on which up to 11 frames holding thin foils may be mounted. The wheel is selsyn-operated from remote stations at either the base of the accelerator (where a viewing port in the tube is located) or from the control console. The aperture for beam passage through the wheel is flanked by permanent magnets to suppress secondary electrons. The position of this section results in a final energy of 1.58 and 2.16 times the terminal voltage for doubly and triply charged ions, respectively.

The target chamber used in this experiment has been previously described in some detail.[14] The chamber is inclined 20.5° from the horizontal, which allows observation of reaction products from 0–139° (lab), with an accuracy in angle settings of $\pm 0.2°$. Previous checks

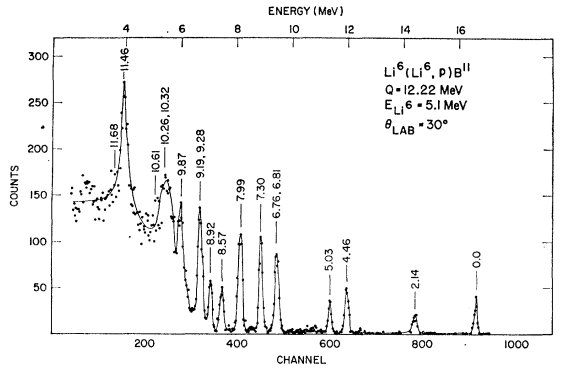

FIG. 2. Energy spectrum of protons from $Li^6(Li^6,p)B^{11}$. The abscissa is marked by channel number and particle energy. Excitation energies in MeV above each peak are taken from Ref. 31.

[9] D. Kurath, Phys. Rev. **101**, 216 (1956).
[10] A. B. Clegg, Nucl. Phys. **38**, 353 (1962).
[11] J. W. Olness, E. K. Warburton, D. E. Alburger, and J. A. Becker, Phys. Rev. **139**, B512 (1965).
[12] G. C. Morrison, Phys. Rev. Letters **5**, 565 (1960).
[13] J. B. Marion and M. Wilson, Nucl. Phys. **77**, 129 (1966).
[14] K. G. Kibler, M.S. thesis, University of Iowa, 1964 (unpublished).

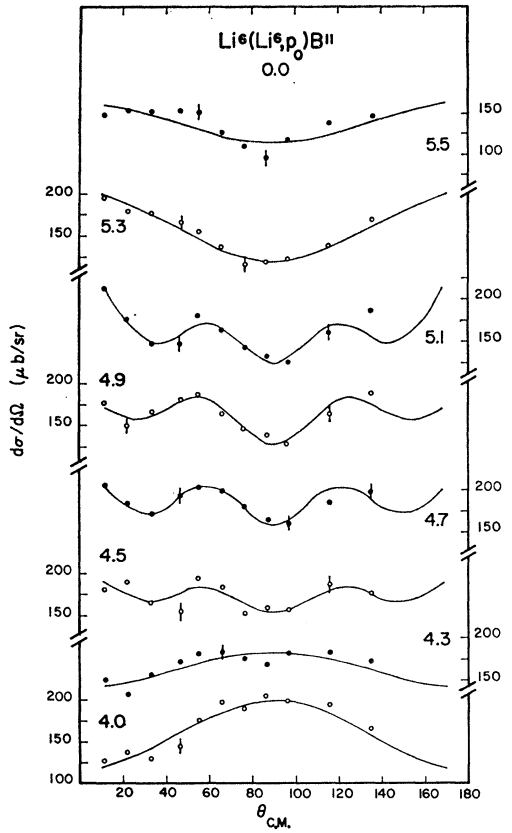

FIG. 3. Angular distributions of protons from $Li^6(Li^6,p_0)B^{11}$. The number near the top center of the figure gives excitation energy of the residual nucleus in MeV. Zero levels are suppressed and the ordinate numbers on the left and right correspond to open and solid plotted points, respectively. The numbers near each curve correspond to bombarding energy. The error bars are statistical only, and the solid curves through the data points represent least-squares fits with Legendre polynomials.

for symmetry and alignment yielded quite satisfactory results. Reaction particles were detected by a system with a proportional counter and a solid-state detector, which was mounted in the movable top of the chamber. A foil wheel with positions for eight foils could be rotated in front of the entrance window of the proportional counter to keep out scattered beam. A 0.0001-in. Mylar foil over the entrance window easily maintains the gas pressure in this counter at the 0.1–0.2 atmospheres used in this experiment. The energy detector (mounted in the gas counter) was a lithium-drifted silicon type, with a 1-cm² sensitive area and a 2000-μ depletion depth at 150-V bias. A smaller surface-barrier detector was fixed in the stationary part of the chamber at 90° to the beam direction, and was used for normalization between runs at a given beam energy.

The targets used in this experiment were lithium-6 fluoride. For yield curves and the angular distribution at 7.35 and 9.0 MeV, the targets were evaporated on self-supporting carbon backings. For all other data, target backings of 1.7 mg/cm² Al were used. The thickness of the targets was determined by using the $(HHH)^+$ beam to measure the $F^{19}(p,\alpha\gamma)$ resonance at 0.872 MeV. From the experimental resonance width, the LiF thickness was determined to be 15.2±0.5 to 872-keV protons. The effective target thickness is 1.4 times this value because the targets were oriented at 45° to the beam. According to the atomic and molecular stopping-cross-section data of Whaling,[15] this thickness is equivalent to 64.3 μg/cm², giving 23.0±2.3 μg/cm² for the effective Li thickness. Extrapolation of Allison's results[16] gives an effective target thickness of about 100 keV for the LiF to a 5.0-MeV Li^6 beam.

The electronics for handling the E (solid-state detector) and ΔE (proportional counter) pulses have been fully described previously.[17] The data are stored in records of 64 E-ΔE pairs on magnetic tape for later analysis, while a continuous live-oscilloscope display

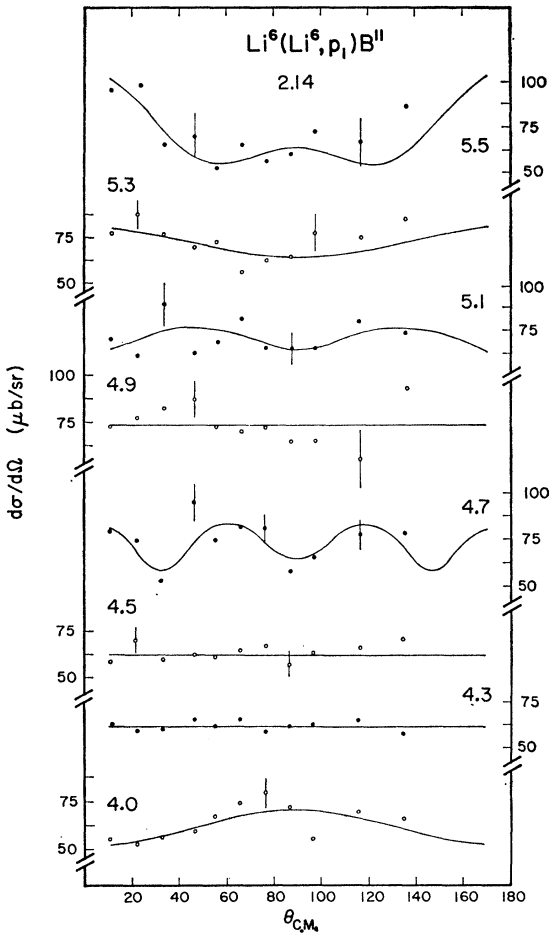

FIG. 4. Angular distribution of protons from $Li^6(Li^6,p_1)B^{11}$. See caption for Fig. 3.

[15] W. Whaling, in *Handbuch der Physik*, edited by S. Flügge (Springer-Verlag, Berlin, 1958), Vol. XXXIV, p. 193.
[16] S. K. Allison, D. Auton, and R. A. Morrison, Phys. Rev. **138**, A688 (1965).
[17] R. R. Carlson and E. Norbeck, Phys. Rev. **131**, 1204 (1963).

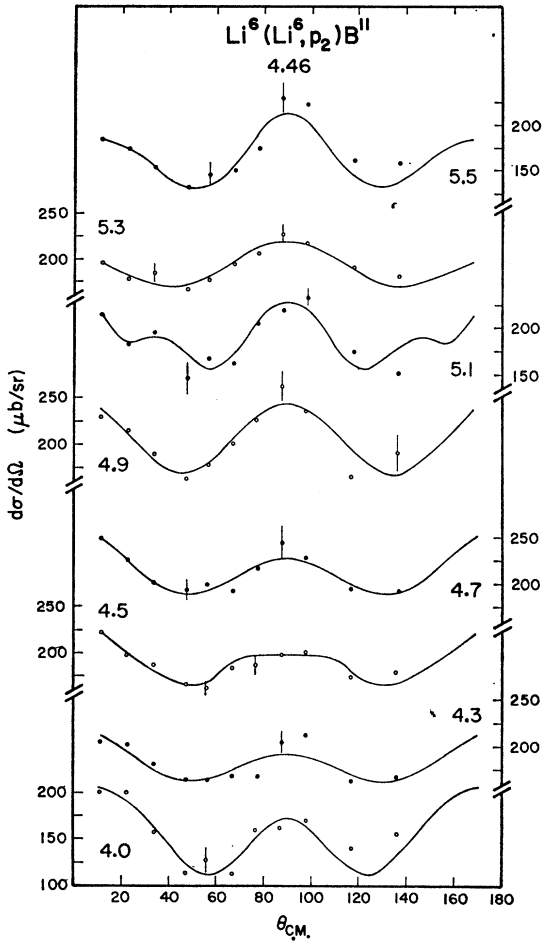

FIG. 5. Angular distributions of protons from $Li^6(Li^6,p_2)B^{11}$. See caption for Fig. 3.

(1024×1024 channels condensed to 128×60) is available during data accumulation. After the data have been collected, a self-consistent set of computer programs is used for analysis in the following manner:

(1) The original data in E, ΔE format are scanned, and the product $(E+C)(\Delta E)$ is taken, where C is an arbitrary constant; the new format E, $(E+C)(\Delta E)$ is written on magnetic tape.

(2) A section of the rewritten, multiplied data containing all charge-1 groups is scanned with full detail in the new ΔE direction; these data are marked with a light pen on the oscilloscope screen to select different-mass particles.

(3) The tape is scanned again and energy spectra for each particle mass are displayed.

(4) Integration under peaks with provision for background subtraction is performed.

The absolute differential cross sections were obtained by normalizing the results at each energy to the average cross section of d_1 obtained from several runs with standard techniques of integration. Relative errors assigned to the differential cross sections total 10%, including repeatability of excitation curves, integrator drift, and statistics. Absolute errors in the total cross sections are assigned to be 20%, which includes target thickness, Li equilibrium charge, integrator calibration, and solid-angle effects.

PROTONS: RESULTS

A typical proton spectrum is shown in Fig. 2. A noticeable continuum is evident in the lower energy region beginning at about 8.6-MeV excitation in B^{11}, the energy at which B^{11} is unbound to $Li^7+\alpha$. Possible reactions contributing to this continuum are

$$Li^6+Li^6 \rightarrow Li^7+He^4+p+3.542 \text{ MeV}$$
$$\rightarrow 2He^4+t+p+1.078 \text{ MeV}$$
$$\rightarrow Be^{10}+2p+0.977 \text{ MeV}.$$

Because of the difficulty of analyzing peaks in this region, no states above 9.3 MeV excitation are reported. Other peaks above this energy are quite evident in the figure, particularly the strong 11.46-MeV state, but the situation in this figure is somewhat unusual. At many

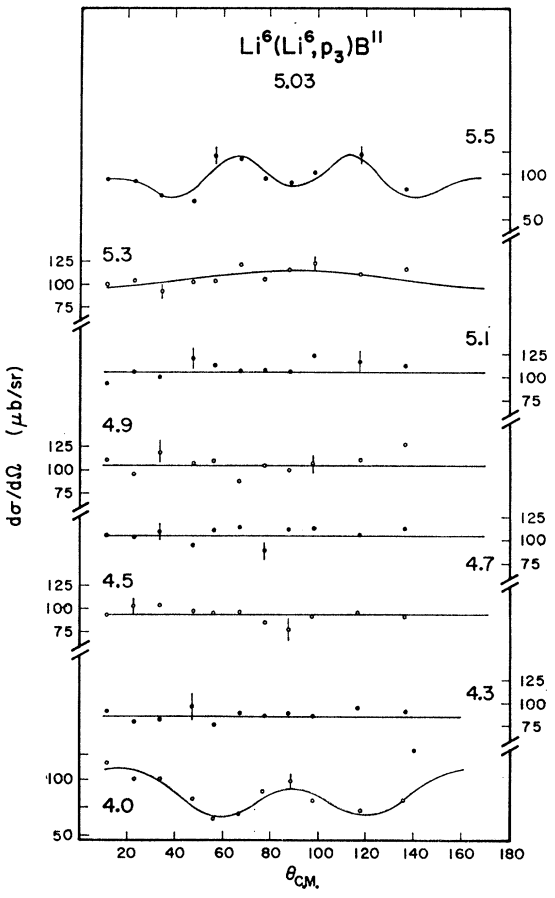

FIG. 6. Angular distributions of protons from $Li^6(Li^6,p_3)B^{11}$. See caption for Fig. 3.

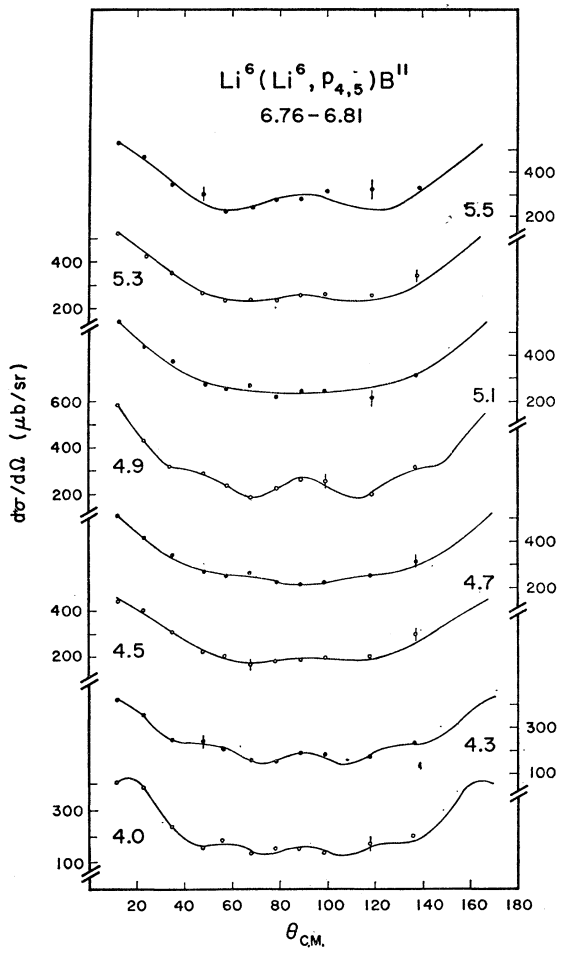

FIG. 7. Angular distributions of protons from $Li^6(Li^6,p_{4,5})B^{11}$. See caption for Fig. 3.

angles, these peaks were barely noticeable above the continuum, but other states not seen here were prominent.

The angular distributions for the protons are shown in Figs. 3 through 12. The solid curves drawn represent least-squares fits to the data with even-order Legendre polynomials. The fits were executed with a χ^2 test for $P=0.05$ (P equals the probability that a larger χ^2 will be obtained in another trial), with the auxiliary condition that $L=10$ was the highest order polynomial used. Satisfactory fits were usually obtained with lower order polynomials, however. If the fits were satisfactory in the χ^2 sense, the total cross sections were taken to be $4\pi A_0$, where A_0 is the coefficient of the zeroth order Legendre polynomial. In some cases when the fit was not satisfactory, a $\sin\theta$-weighted integration was performed using a trapezoidal rule. The cross sections as computed by these alternative methods were found to agree within statistics.

Proton data are not presented at the three lowest (2.4, 2.8, and 3.2 MeV) and two highest (7.35 and 9.0 MeV) energies. In these regions either the statistics were prohibitively bad or the experimental conditions were arranged to maximize detail in particular energy regions of the deuteron spectra, for example. The data at the two highest energies resulted in total cross sections which were the same (within statistics) as those at 5.5 MeV. The proton angular distributions at 7.35 and 9.0 MeV were either the same shape for most groups as those at 5.5 MeV, or were nearly isotropic. At these two high energies, interference in the proton spectra from contaminant reactions was often noticeable, and thus some of the proton results with regard to both total cross sections and angular distributions had to be obtained from a limited number of data (3–6 angles in many cases).

The proton angular distributions for incident energies from 4.0 to 5.5 MeV exhibit significant variations as the energy is increased, but for some groups the shape changes smoothly or is relatively constant with minor fluctuations over this energy range. From the Legendre polynomial fits, the ratios A_L/A_0 (ratio of Lth-order coefficient to zeroth-order coefficient) were also obtained. By examining these ratios as a function of energy, one eliminates to some extent the effect of rapidly

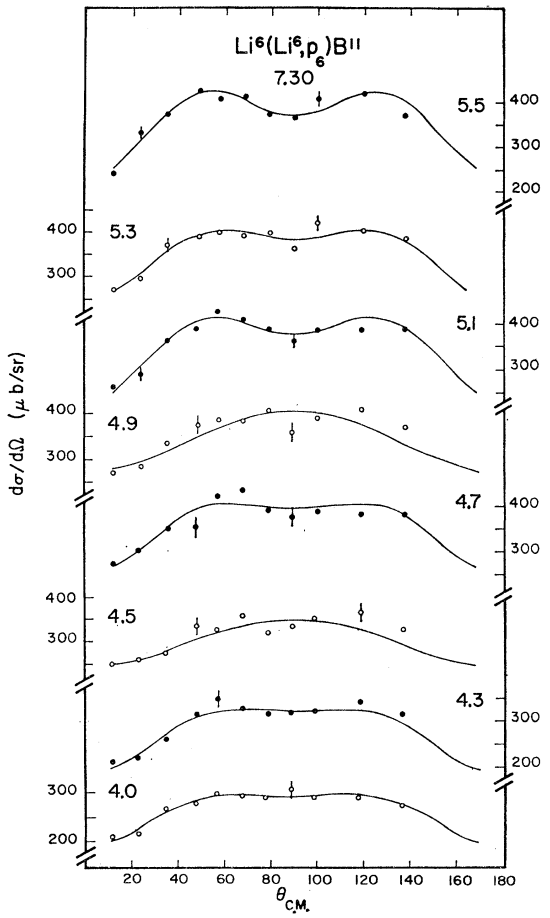

FIG. 8. Angular distributions of protons from $Li^6(Li^6,p_6)B^{11}$. See caption for Fig. 3.

changing penetrabilities. These ratios show, as did the angular distributions, noticeable variations in the shape of the differential cross sections as a function of incident energy. These variations are not particularly abrupt from energy to energy, however.

Figures 13 and 14 show the yield curves for the protons. The variation in cross section is not the same for all proton groups. For example, p_1 and p_3 are nearly constant over this energy range, while p_0, p_2, p_9, and $p_{10,11}$ show indications of maxima around 4.7 MeV. The largest variation from 4.0 to 5.5 MeV is a factor of about 1.5 for the cross sections for $p_{4,5}$, p_6, p_7, and p_8, for example. In all these latter cases the cross section increases as the incident energy is raised. Within experimental errors, however, there are no indications of strong structure in the proton yield curves from 4.0 to 5.5 MeV.

Compared to the available proton results at 2.1 MeV,[6] the angular distributions at 4.0 MeV are similar for p_0, different for p_1, and somewhat similar for p_3. The total cross sections at 4.0 MeV are typically 3–5 times greater than the corresponding results at 2.1 MeV.

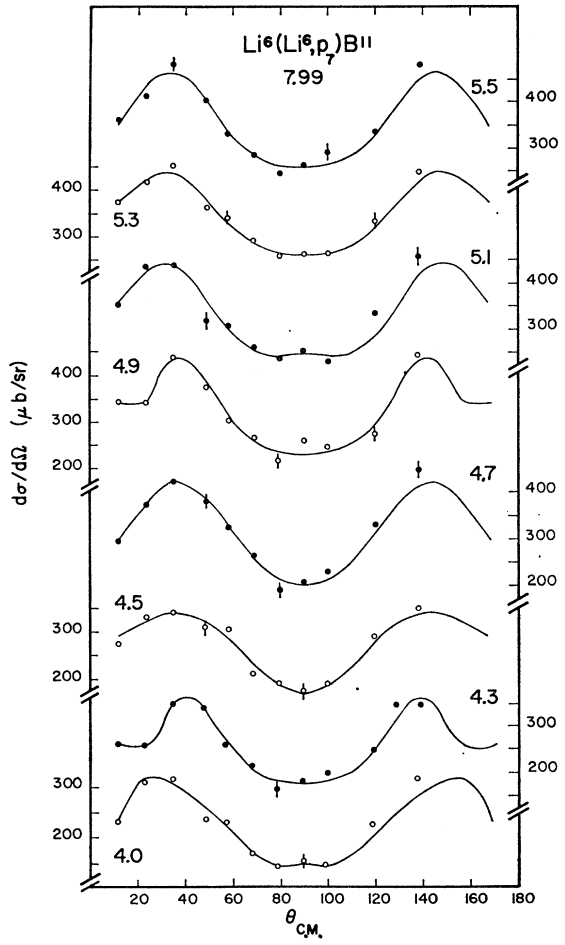

FIG. 9. Angular distributions of protons from $Li^6(Li^6,p_7)B^{11}$. See caption for Fig. 3.

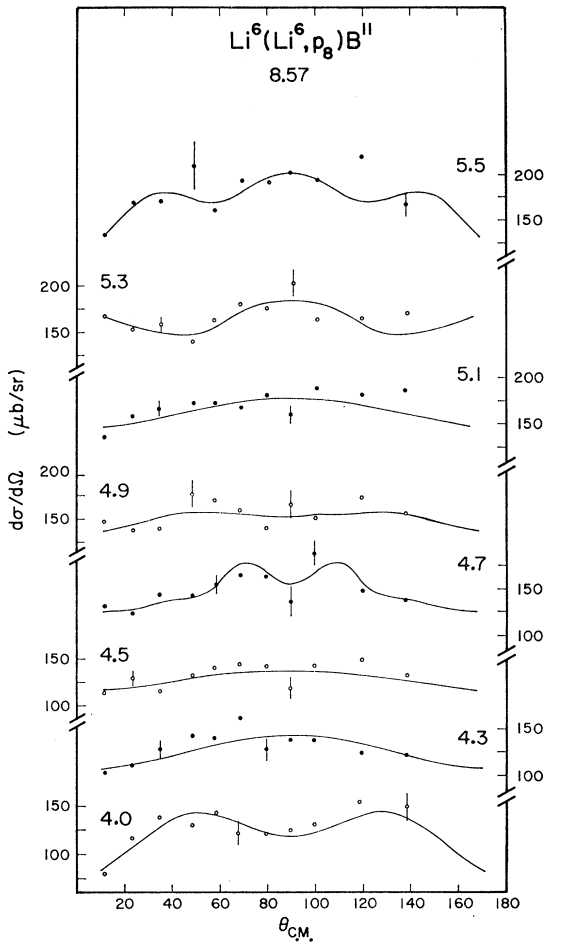

FIG. 10. Angular distribution of protons from $Li^6(Li^6,p_8)B^{11}$. See caption for Fig. 3.

PROTONS: DISCUSSION

The results from Chicago for p_0 to p_3 at 2.1 MeV give typical cross sections for these groups as about 0.5 mb.[6] The present results for these cross sections at 4.0 MeV are 0.8–3.0 mb. One can readily compute the simple barrier-penetration cross section,

$$\sigma_c=\pi\lambda\!\!\!^{-2}\sum(2L+1)T_L,$$

using standard penetrability tables.[18] For $L=0$ to $L=3$, we find

$$\sigma_c\simeq 30 \text{ mb at } 2.1 \text{ MeV}$$
$$\simeq 150 \text{ mb at } 4.0 \text{ MeV}$$
$$\simeq 225 \text{ mb at } 5.5 \text{ MeV}.$$

The experimental change in proton cross sections between 2.1 and 4.0 MeV is well described by the factor of 5 given by this calculation. For those proton cross sections which increase from 4.0 to 5.5 MeV, we previ-

[18] W. T. Sharp, H. E. Gove, and E. B. Paul, in Atomic Energy Commission, Limited, Report No. AECL 268, 1965 (unpublished).

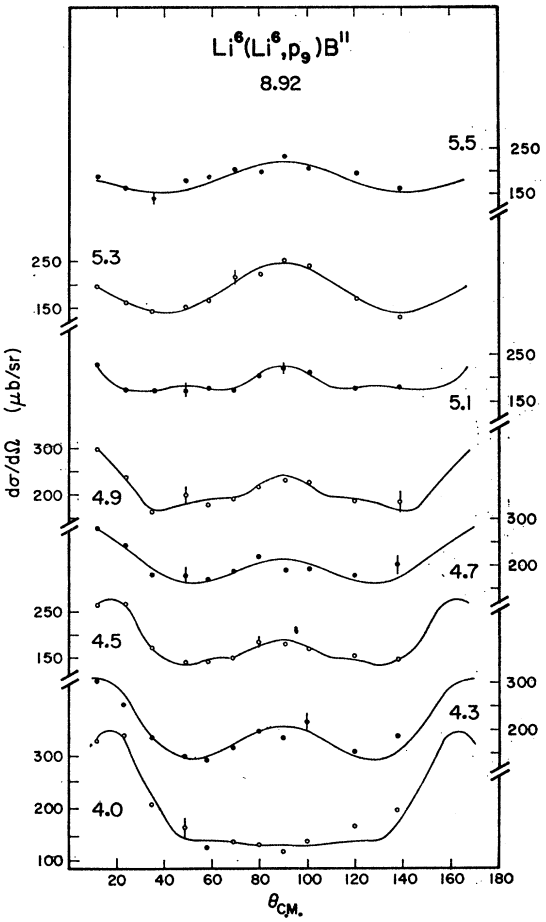

FIG. 11. Angular distributions of protons from $Li^6(Li^6,p_9)B^{11}$. See caption for Fig. 3.

ously mentioned that the increase was typically a factor of 1.5, which again is in agreement with the values just calculated.

An important exit channel with respect to the present proton results is the $C^{11}+n$ possibility. Angular distributions for the proton groups at 4.0 MeV compare quite well in shape with neutron results at 4.1 MeV.[19] If we assume the neutron cross sections are roughly equal to the proton values, then the total $(p+n)$ cross section at 4.0 MeV is about 50 mb, and accounts for $\frac{1}{3}$ of σ_c. A direct reaction mechanism for these groups would be difficult to reconcile with the angular distribution agreement. For the (Li^6,p) and (Li^6,n) cases, either a He^5 or a Li^5 must be transferred. Although the He^5+p threshold in Li^6 is only 4.6 MeV, the large Coulomb effects accompanying such many-nucleon transfers would render unlikely the similarity of proton and neutron angular distributions in such a case. Previous mention of evidence for He^6+p clustering in Li^6 has been made,[20] and the separation energy is not high enough to negate this possibility entirely. The smooth yield curves and relatively unchanging angular distributions for some proton groups lead one to suspect a non-negligible amount of direct process, but the compound nucleus must still be the dominant mechanism.

In the yield curves for p_0, p_2, p_9, and $p_{10,11}$ we previously noted slight indications of maxima around 4.7 MeV. We might point out that the Hauser-Feshbach results[21] indicate a maximum in statistical compound-nucleus (SCN) cross sections near the Coulomb barrier, but this maximum is usually quite pronounced,[22] in contrast with the slight effect noted here. The previous success of McGrath in interpreting his Li+B results[8] on the basis of an SCN theory provides significant impetus to pursue this in the present experiment.

The large mass excess of Li^6 puts one at 30.2 MeV in the C^{12} compound nucleus at 4.0-MeV incident energy. Calculations of level densities in this region, using the

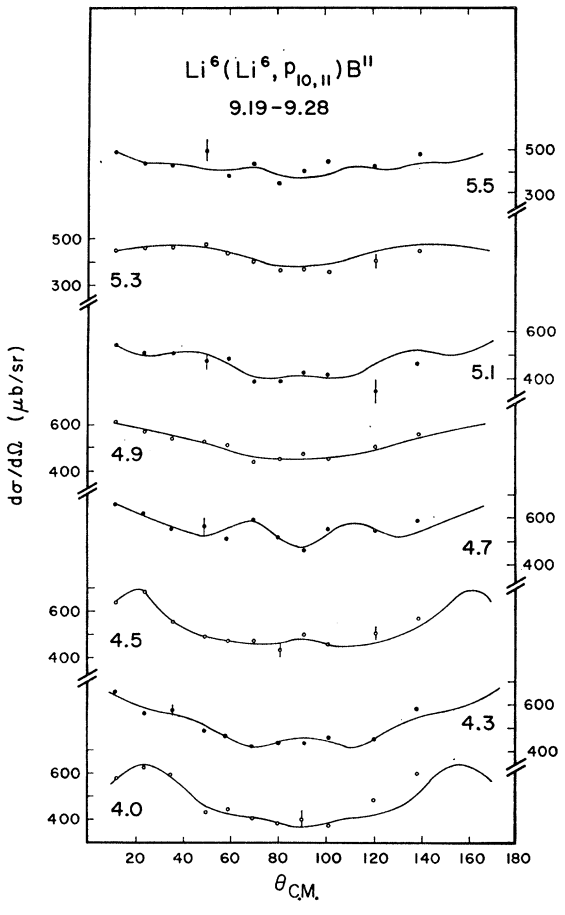

FIG. 12. Angular distributions of protons from $Li^6(Li^6,p_{10,11})B^{11}$. See caption for Fig. 3.

[19] R. M. Bahnsen, Ph.D. dissertation, University of Iowa, 1966 (unpublished).

[20] G. C. Morrison, in *Proceedings of the Third Conference on Reactions Between Complex Nuclei*, edited by A. Ghiorso, R. M. Diamond, and H. E. Conzett (University of California Press, Berkeley, California, 1963), p. 197.

[21] W. Hauser and H. Feshbach, Phys. Rev. **87**, 366 (1952).

[22] Y. Cassagnou, I. Iori, C. Levi, T. Mayer-Kuckuk, M. Mermaz, and L. Papineau, Phys. Letters **7**, 147 (1963).

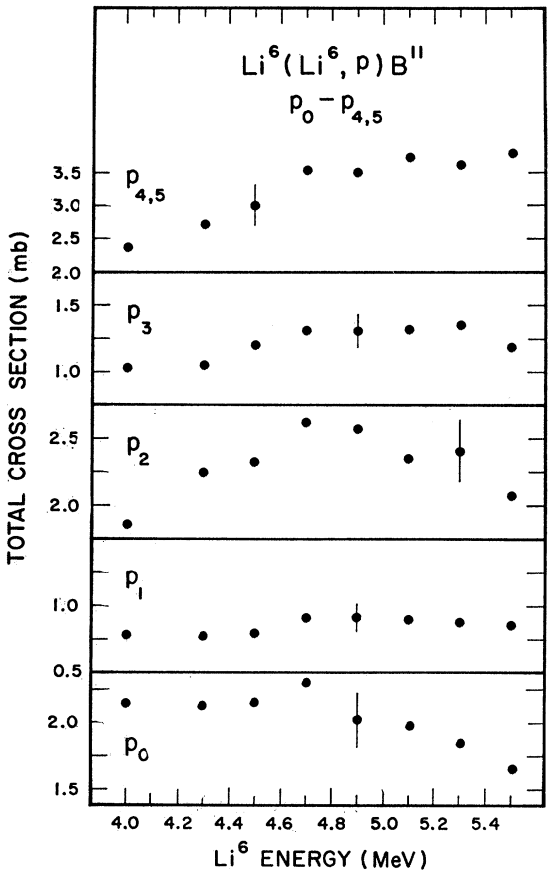

FIG. 13. Total cross sections for p_0 to $p_{4,5}$. Typical relative errors indicated by error bars. Note suppressed zero levels. Absolute scale has error of ±20%.

formula of Lang,[23] indicate that one is justified in attempting a consideration of the proton results from an SCN viewpoint. At 30.2 MeV in C^{12}, the calculated width (Γ) is 110 keV. This Γ is the calculated neutron width,[24] so the actual width should reasonably be considerably larger. Legge and Bubb have studied C^{12} in the 20.5–26.5-MeV excitation region via an activation technique with $B^{11}(p,n)C^{11}$.[25] They see definite peaks in the cross section with Γ always greater than 70 keV.

To justify application of SCN concepts we should be in the region of overlapping levels for a particular spin-parity. For spins 0, 1, 2, and 3, and either parity, we find Γ/D equals 2, 3, 1.5, and 0.5, respectively. Thus although Γ/D is not necessarily much greater than unity for a given spin-parity, we are probably in the region of overlapping levels. With this result and other conditions not generally too restrictive,[26] if the mechanism is compound nucleus we expect the total cross sections to be proportional to $(2J+1)$, where J is in this case the spin of the particular B^{11} residual level considered.

Figures 15 and 16 show the proton cross sections plotted versus $2J+1$ of the B^{11} states. In Fig. 15, the cross sections are averaged over 8 incident energies, so that $\Delta E \gg \Gamma$, but the $2J+1$ dependence is not good. The general trend is that this dependence improves with increasing incident energy (i.e., higher C^{12} excitation) but is really good only at 5.5 MeV, as shown in Fig. 16. We may really be just entering the statistical region at this energy, but with good results at only one energy, the agreement may be fortuitous. The $2J+1$ dependence of proton results at 7.35 and 9.0 MeV is not good, although we should certainly be in a statistical region of C^{12} at these bombarding energies. The previously mentioned large statistical errors for these high-energy results, due to both the low yield and the limited angular range of data, may be the cause for such disagreement.

If one takes a suitable energy average so that $\Delta E \gg \Gamma$, the differential cross sections are expected to be symmetric about 90°. This is of course not noticeable here because of the particle identity in the entrance channel.

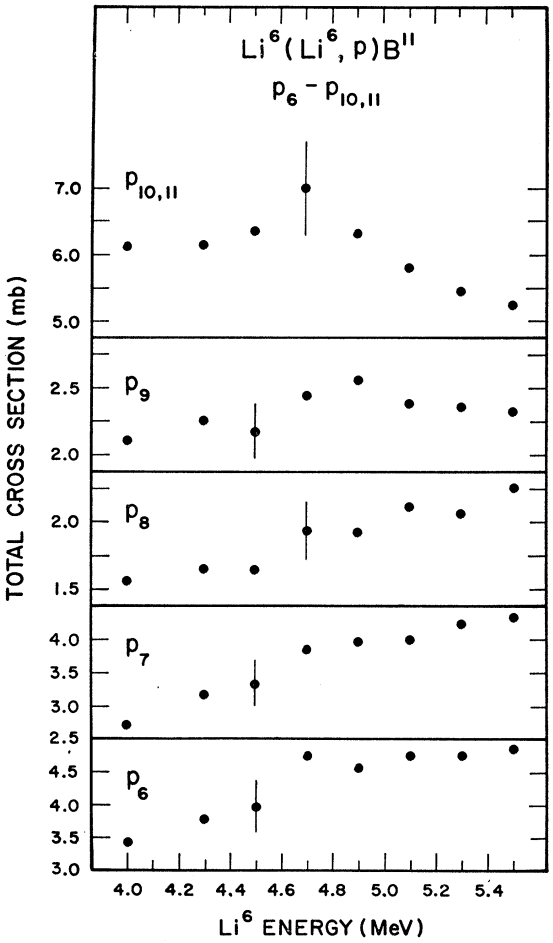

FIG. 14. Total cross sections for p_6 to $p_{10,11}$. See caption for Fig. 13.

[23] D. Lang, Nucl. Phys. **26**, 434 (1961).
[24] T. Ericson, Ann. Phys. (N. Y.) **23**, 390 (1963); Advan. Phys. **9**, 425 (1960).
[25] G. J. F. Legge and I. F. Bubb, Nucl. Phys. **26**, 616 (1961).
[26] N. McDonald, Nucl. Phys. **33**, 110 (1962).

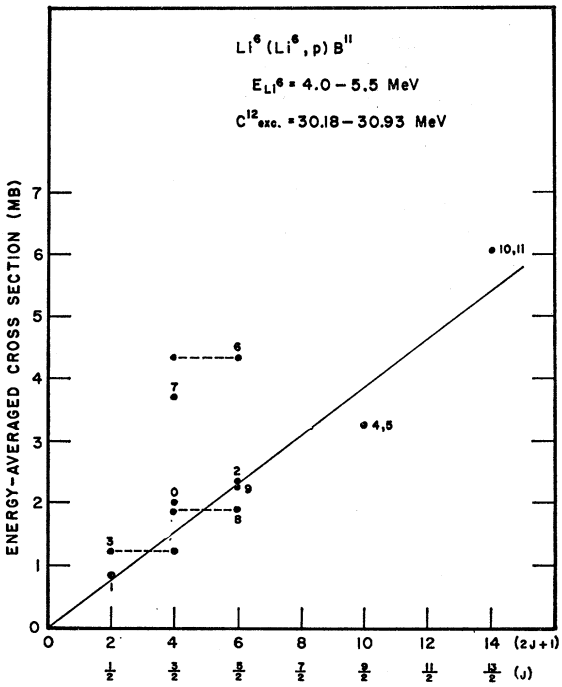

FIG. 15. B^{11} total cross section in mb versus $2J+1$ values. The cross sections are averaged over eight bombarding energies between 4.0 and 5.5 MeV. Points are plotted for best $2J+1$ dependence. Dashed lines connect points where spin is uncertain and $2J+1$ dependence is similar for both spins. See Fig. 16 for spins of B^{11} levels.

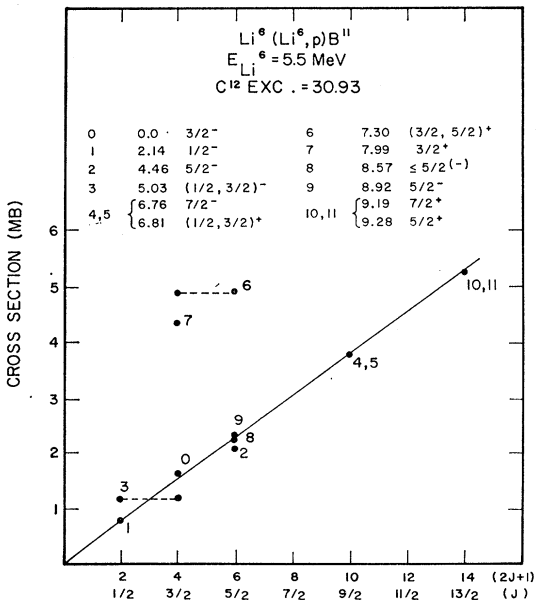

FIG. 16. B^{11} total cross sections in mb versus $2J+1$ values. These cross sections are taken at 5.5-MeV Li^6 energy. Points are plotted for best $2J+1$ dependence. Dashed lines connect points where spin is uncertain and $2J+1$ dependence is similar for both spins.

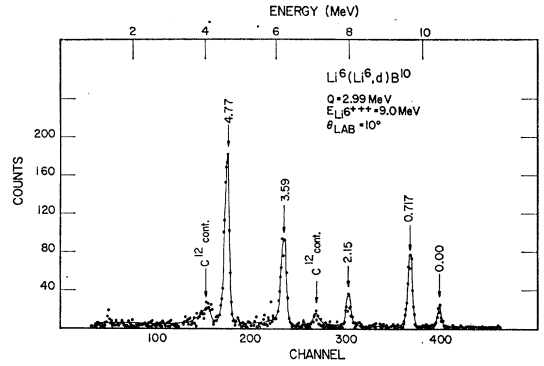

FIG. 17. Energy spectrum of deuterons from $Li^6(Li^6,d)B^{10}$. See caption for Fig. 2.

We do note that the differential cross sections show more variation than the integrated values, but this effect is expected, from angular-momentum considerations for example.[24]

One can note that in both Figs. 15 and 16, the cross sections for p_6 and p_7 are far above the $(2J+1)$ line.

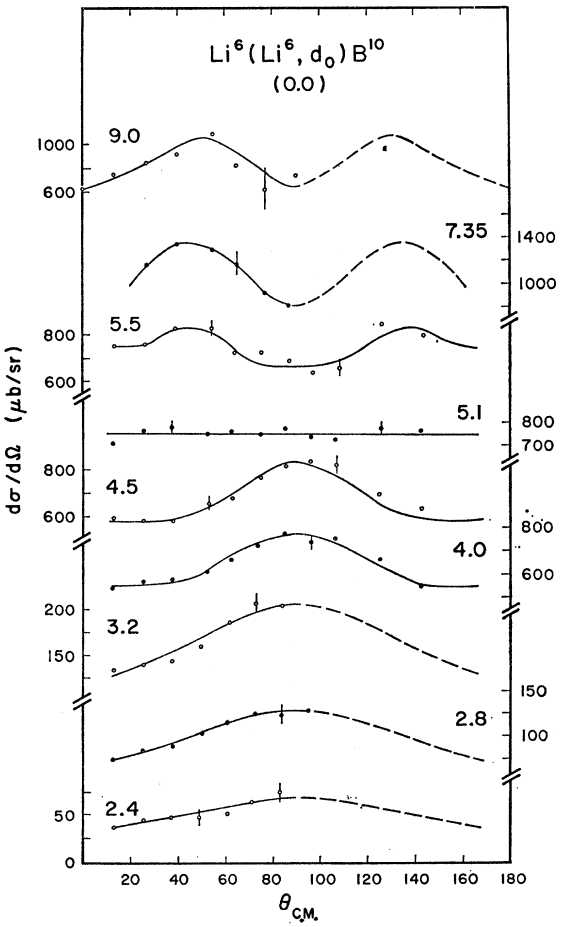

FIG. 18. Angular distributions of deuterons from $Li^6(Li^6,d_0)B^{10}$. Bombarding energy range is 2.4–9.0 MeV. Figure 19 shows 4.0–5.5-MeV energy range in greater detail. See caption for Fig. 3.

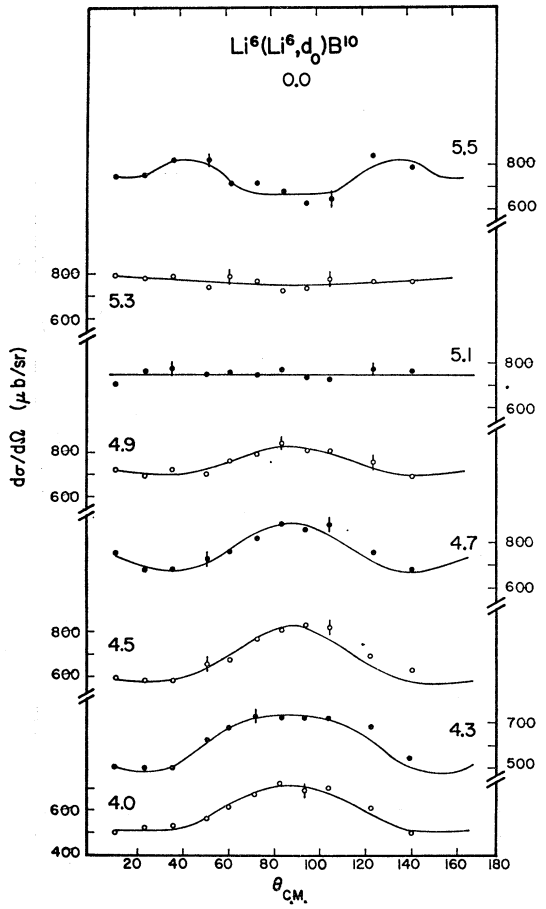

FIG. 19. Angular distributions of deuterons from $Li^6(Li^6,d_0)B^{10}$. Bombarding energy range is 4.0–5.5 MeV. See caption for Fig. 3.

In comparisons of the proton and neutron[19] data from this reaction, the angular distributions for those two states disagreed to the largest extent with the C^{11} mirror states. In the Li+B case of McGrath,[8] disagreements with $2J+1$ were typically to the high side, as is the case here. Berkowitz *et al.*[27] also noted from γ-ray data that these two states had an unusually large population at lower bombarding energy.

The origin of these two even-parity states is not as well known as that of the odd-parity ones in B^{11}. Both intermediate-coupling[9] and unified-model[10] calculations account reasonably well for the first five odd-parity levels assuming an s^4p^7 configuration, if one is allowed some freedom in the a/K parameter in Kurath's results.[9] The even-parity levels are more complicated however. The states at 9.19 and 9.28 MeV are adequately explained by the weak coupling of a $2s_{1/2}$ nucleon to the B^{10} ground state.[11] The levels at 6.81, 7.30, and 7.99 MeV have very small reduced widths for this coupling, however.[28] If these states arise from a p^6s or p^6d configuration, the B^{10} ground state does thus not appear to be the major parent. In mass-11 nuclei, the $2s_{1/2}$ shell is lower than the $1d_{5/2}$, so p^6s is more likely than p^6d for these states.[28] As Olness *et al.*[11] point out, the weak coupling of a $2s_{1/2}$ nucleon to the first excited state of B^{10} (1+) can account for two of these states; either the 7.30- or the 7.99-MeV state would then have a higher B^{10} level for its core. These states at 7.30 and 7.99 MeV are weakly excited in (d,p) work,[29] although states such as those at 6.76 and 8.92 MeV are strongly formed, which substantiates the more complicated configurations of the 7-MeV states. The 9.19–9.28-MeV doublet agrees well with $2J+1$, and the 6.76–6.81 doublet agrees if the lower spin ($\frac{1}{2}^+$) is chosen for the positive-parity 6.81-MeV level. The 5.03-MeV state fits equally well in Fig. 16 with spin $\frac{1}{2}$ or $\frac{3}{2}$, but the 8.57-MeV state [$\leq\frac{5}{2}^{(-)}$] fits best a choice of $\frac{5}{2}$ for its spin.

If the $(2J+1)$ dependence of the proton cross sections at 5.5 MeV is indeed meaningful, then some basic

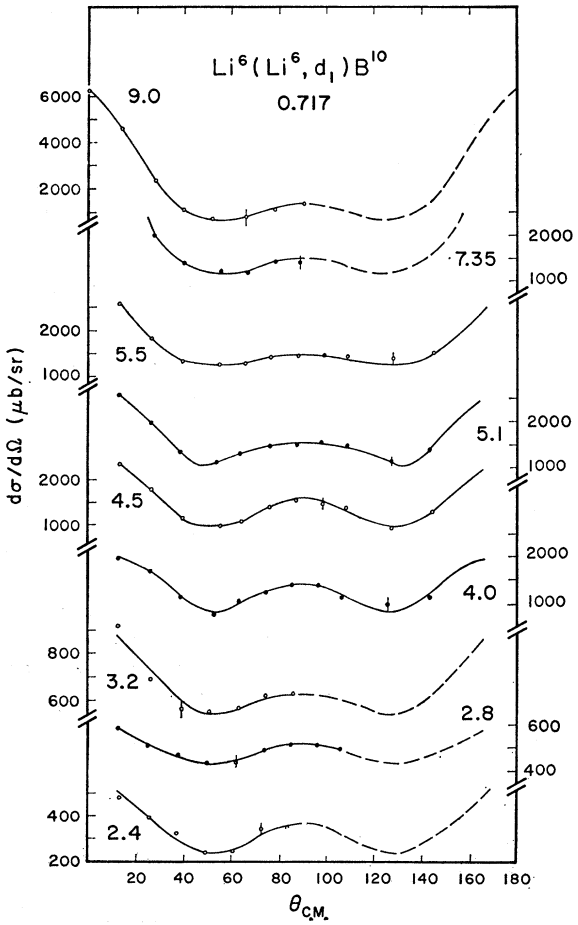

FIG. 20. Angular distributions of deuterons from $Li^6(Li^6,d_1)B^{10}$. Bombarding energy range is 2.4–9.0 MeV. Figure 21 shows 4.0–5.5-MeV energy range in greater detail. See caption for Fig. 3.

[27] E. Berkowitz, S. Bashkin, R. R. Carlson, S. A. Coon, and E. Norbeck, Phys. Rev. **128**, 247 (1962).
[28] I. Talmi and I. Unna, Ann. Rev. Nucl. Sci. **10**, 353 (1960).
[29] S. Hinds and R. Middleton, Nucl. Phys. **38**, 114 (1962); O. M. Bilaniuk and J. C. Hensel, Phys. Rev. **120**, 211 (1960).

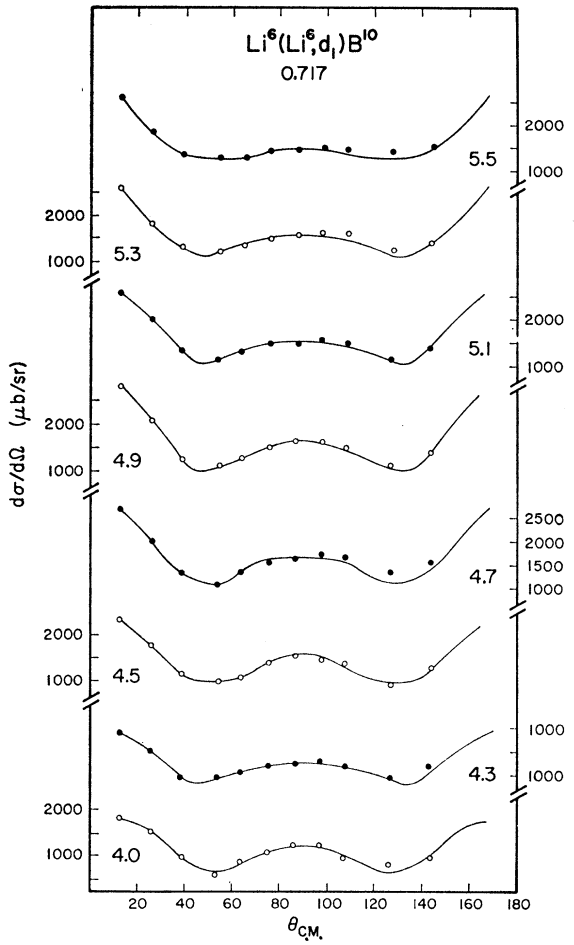

FIG. 21. Angular distributions of deuterons from $Li^6(Li^6,d_1)B^{10}$. Bombarding energy range is 4.0–5.5 MeV. See caption for Fig. 3.

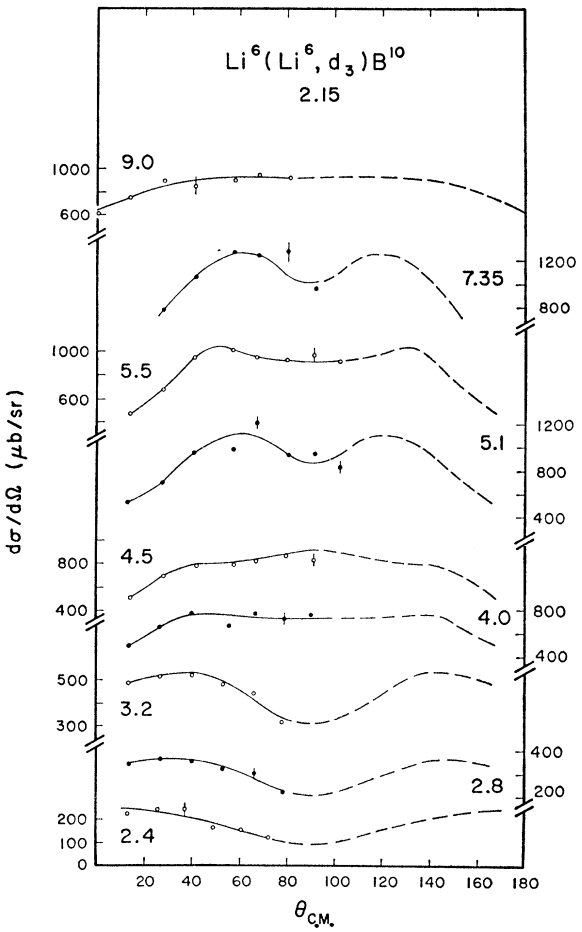

FIG. 22. Angular distributions of deuterons from $Li^6(Li^6,d_3)B^{10}$. Bombarding energy range is 2.4–9.0 MeV. Figure 23 shows 4.0–5.5-MeV energy range in greater detail. See caption for Fig. 3.

difference between the 7.30- and 7.99-MeV states and the other B^{11} levels is indicated. Perhaps the large yield reflects a significant contribution from a direct mode of formation. We note that the good agreement with $(2J+1)$ for the odd-parity levels may just reflect their similar configurations. Direct-reaction modes also contain a $(2J+1)$ dependence which results from a summation over magnetic substates of the DR transition amplitude, but this dependence is usually negligible compared to the greater influence of reduced widths in determining the total cross section to particular final states. If, however, the residual level configurations are similar, then the $(2J+1)$ factor may dominate. A significant direct-reaction contribution in the proton results thus cannot be ruled out. The evidently complicated configurations of the 7.30- and 7.99-MeV states, and the high yields to these levels, may well indicate strong formation by a direct 5-nucleon transfer. This then could account for the less-satisfactory agreement between these levels and the mirror C^{11} states, since Coulomb effects would be important.

DEUTERONS: RESULTS

Figure 17 shows a typical deuteron spectrum. One notes the absence of the 1.74-MeV state (0^+, $T=1$) in agreement with previous discussions.[12] The deuteron spectra are quite free of contaminant groups except at the higher energies (7.35 and 9.0 MeV), where carbon-backed targets were used because of many complications from Li^6+Al reactions on the Al backings used at lower energies. The groups from Li^6+C^{12} were fairly prominent but in most cases did not obscure relevant data of interest.

Angular distributions for d_0, d_1, d_3, d_4, and d_5 are shown in Figs. 18 through 24. As was the case for the protons, the curves represent least-squares fits with even-order Legendre polynomials. The cross sections were then taken from A_0 if such a fit was satisfactory according to χ^2, or from a numerical integration otherwise. The only energies at which relatively complete data could be obtained for d_4 and d_5 were for the two highest energy runs.

The d_0 angular distribution changes quite noticeably over the entire energy range. At the low end, the results are very similar in shape to those of the Chicago group.[6] As the incident energy is raised, the shape undergoes a fairly smooth transition in the Coulomb-barrier region and becomes peaked at about 40° and thus at 140° also. This shape is retained up to the highest energy studied, and agrees quite well with the Argonne results[5] in this region. In fact, the run at 7.35 MeV is, as mentioned previously, at the same center-of-mass energy as the 8.0-MeV Argonne data. Figure 25 shows a comparison of results at this energy. The inverse reaction data have been converted to the Li^6+Li^6 incident channel via detailed balance. The agreement is quite good with respect to shape, and very reasonable with regard to absolute values, considering the 20% statistics assigned here.

The d_1 results in Fig. 18 are somewhat different. The general shape is retained throughout the energy range studied, but the forward peak increases noticeably with increasing energy. The curve at 2.4 MeV agrees well with the Chicago work at 2.1 MeV. The angular distributions for d_3 are fairly constant in shape in the regions above and below 4.0 MeV, with a transition occurring between 3.2 and 4.0 MeV.

Figure 26 summarizes the behavior of the cross sections for d_0, d_1, and d_3 as a function of incident energy. Within statistics, the curves are smooth and similar for these groups. For comparison purposes, the total cross sections for d_4 and d_5 at 9.0 MeV are 24 and 35 mb, respectively—noticeably higher than for the other groups.

DEUTERONS: DISCUSSION

The cross section for even the lowest yield deuteron, d_0, is typically 3–4 times greater than an average proton value at 4.0 MeV, which suggests a different mechanism of formation for B^{10} as opposed to B^{11} in this reaction. In fact the sum of the first three measured deuteron cross sections is greater than that for 11 protons, even though the most energetic deuterons have only about 6 MeV, compared with 15 MeV for the protons.

As previously mentioned, the shape of the d_0 angular distribution at 2.4 MeV compares well with previous 2.1-MeV results,[6] but an extrapolation of the present yield curve to 2.1 MeV suggests that the absolute values disagree by 50%. As the incident energy increases,

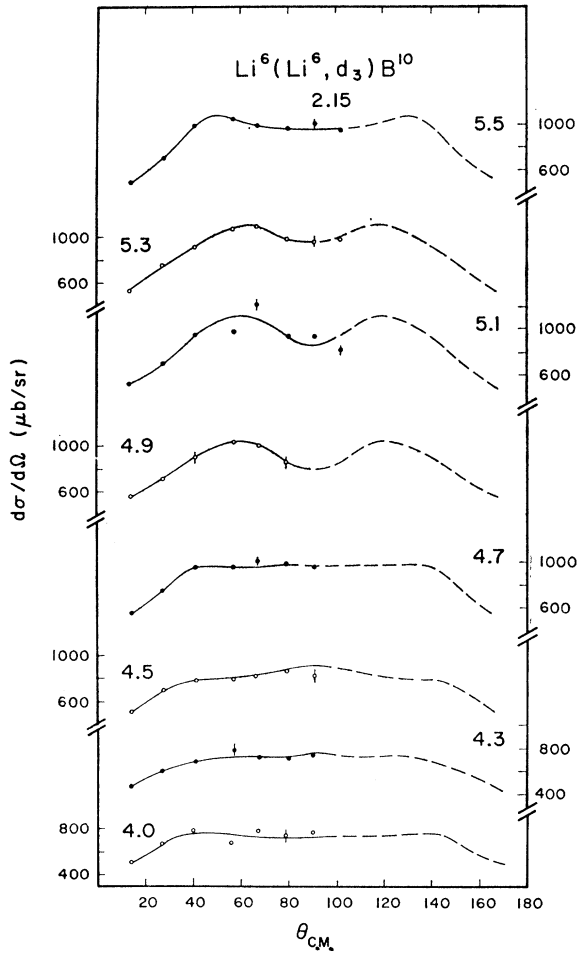

FIG. 23. Angular distributions of deuterons from $Li^6(Li^6,d_3)B^{10}$. Bombarding energy range is 4.0–5.5 MeV. See caption for Fig. 3.

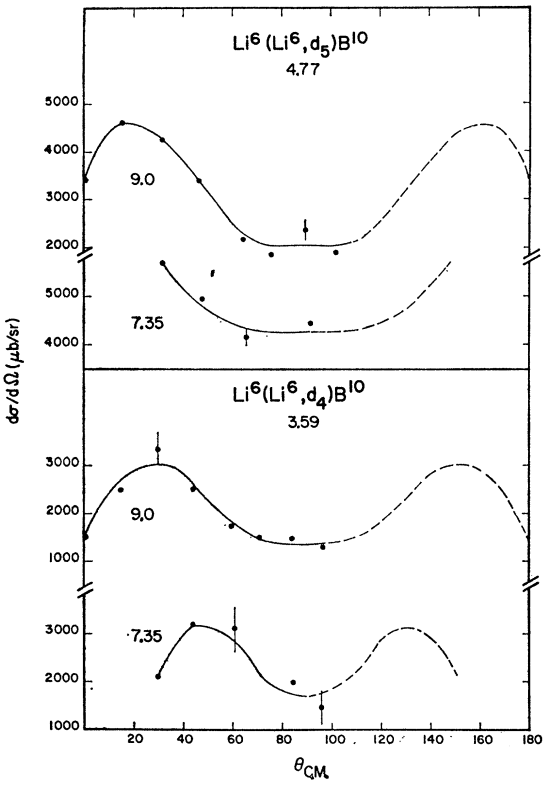

FIG. 24. Angular distributions of deuterons from $Li^6(Li^6,d_4)B^{10}$ and $Li^6(Li^6,d_5)B^{10}$ at 7.35- and 9.0-MeV bombarding energy. See caption for Fig. 3.

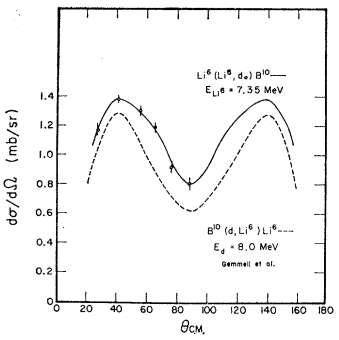

FIG. 25. Angular distribution of deuterons from $Li^6(Li^6,d_0)B^{10}$ and the inverse reaction (Ref. 5). The inverse-reaction data have been converted via detailed balance to the Li^6+Li^6 entrance channel.

however, the angular distribution tends to become quite isotropic near the Coulomb barrier. There is, in fact, an $l=0$, $S=2$ exit channel which would match the $l=0$, $S=2$ entrance channel and possibly result in strong isotropy for the angular distribution if the reaction proceeded by way of a compound nucleus. If, however, one prefers to picture the reaction as proceeding via an α transfer, we must have $l_\alpha=2$ to form the 3^+ B^{10} ground state, and this orbital angular momentum in the entrance channel could account for the peaking at 90° observed below the Coulomb barrier.

We comment briefly here on the relevance of the absence of the 1.74-MeV (0^+, $T=1$) state in the spectrum (Fig. 17). An upper limit on the cross section for formation of this state is 0.3 mb at 4.0 MeV for example, or about 1/30 of the d_0 cross section. The inhibition of this state has been discussed in detail by Morrison.[12] Formation of this state is strictly forbidden by spin considerations if the reaction proceeds via direct α capture. If a compound-nucleus mechanism dominates, formation is inhibited by isospin conservation. The state is greatly inhibited in the $Li^6(Li^7,t)B^{10}$ reaction also,[30] where isospin conservation provides no restriction. The only apparent explanation in this latter case is the inability to form a 0^+ state by α capture of the Li^6. These results would suggest a direct mechanism.

Above the barrier, the d_0 results show a marked peaking at about 40° which persists through the high-energy region. This agrees quite favorably with the inverse-reaction results.[5] Not only are the (Li^6,d) and (d,Li^6) angular distributions identical at the same center-of-mass energy, but Fig. 25 indicates the absolute magnitudes agree to about 20%. Some of the Argonne data were fitted with the distorted-wave Born approximation (DWBA) by Satchler, assuming an $l=2$ alpha transfer, and the results were quite encouraging. One might then say with reasonable assurance that this far above the barrier, the mechanism is dominantly a direct one.

The angular distribution for d_1 is quite constant in shape over the entire energy range, with the only obvious change being the growing prominence of the forward peak as the bombarding energy increases. The cross section for d_1 is typically a factor of 2 greater than that for d_0 in the Coulomb barrier region. The prominent forward peak is suggestive of an $l_\alpha=0$ transfer, and this is indeed a possible formation mode since the first-excited B^{10} state is 1^+.[31] Perhaps the absence of a centrifugal barrier facilitates formation of this state to the extent that the mechanism may be similar throughout the energy range studied.

The third excited state (2.15 MeV) also has 1^+, and could thus be formed via an $l_\alpha=0$ process. The Q value here is only 0.84 MeV, compared with 2.27 MeV for d_1. The similar behavior of the cross section as a function of energy for these two states suggests a similar reaction mechanism, with the nonsimilarity in shape of the angular distributions resulting from differences in the states.

In B^{10}, we are midway through the $1p$ shell, and thus have quite complicated level structure. There are two $p_{3/2}$ nucleons missing from the closed C^{12} shells, so the ground state should correspond to a $(p_{3/2})^2$ configura-

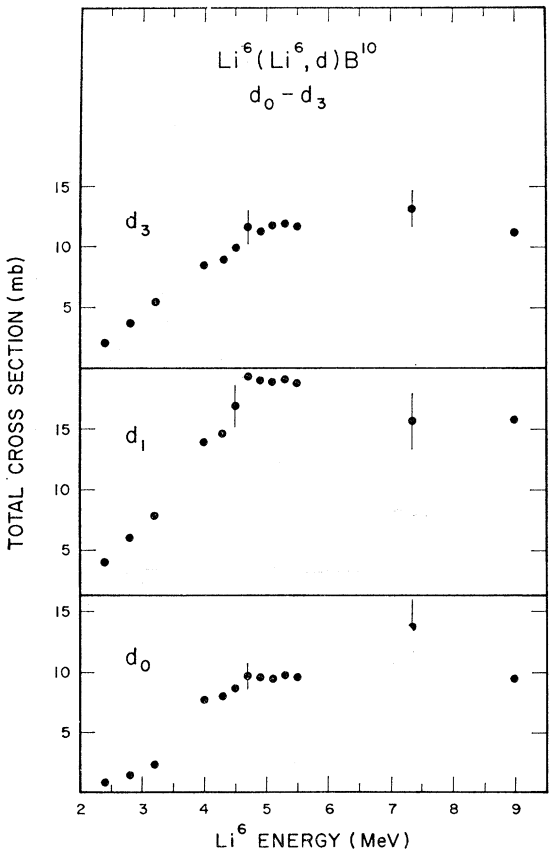

FIG. 26. Total cross sections for d_0, d_1, and d_3. See caption for Fig. 13.

[30] G. C. Morrison and M. N. Huberman, in *Reactions Between Complex Nuclei*, edited by A. Zucker, F. T. Howard, and E. C. Halbert (John Wiley & Sons, Inc., New York, 1960), p. 246.

[31] T. Lauritsen and F. Ajzenberg-Selove, in *Nuclear Data Sheets*, compiled by K. Way *et al.* (Printing and Publishing Office, National Academy of Sciences—National Research Council, Washington, D. C., 1962), NRC 61-5-6; Nucl. Phys. **78**, 1 (1966).

tion. The two lowest states do have $J=3$ and $J=1$, respectively, as expected from this configuration.[28] However, the 2.15-MeV state is also 1^+.[31] As Talmi and Unna point out, this level should lie higher, since it requires the excitation of a $p_{3/2}$ nucleon into the $p_{1/2}$ subshell.[28] These two low-lying 1^+ levels imply that a pure jj-coupling scheme is not satisfactory in this region. The intermediate-coupling calculations of Kurath for mass-10 nuclei, however, show the best agreement with experiment of all the $1p$-shell nuclei.[9] The first six levels are quite adequately accounted for in Kurath's results.

The present experimental results for d_4 and d_5 with regard to differential and total cross sections are very similar. The 3.59-MeV level has $J^\pi=2^+$, and the 4.77-MeV level probably the same.[31] The 4.77-MeV level was once thought to be 1^+, which was troublesome from the point of view of Kurath's calculations, but the probable 2^+ assignment fits well into the intermediate-coupling results.[9] The cross sections for these groups are larger than any of the other deuteron cross sections, and the d_5 result is larger than that for d_4. The proximity of these states to the $Li^6+\alpha$ threshold in B^{10} (4.46 MeV) might well favor their formation by α transfer. The similarity of the angular distributions for d_4 and d_5 suggests both are formed by an $l_\alpha=2$ transfer process.

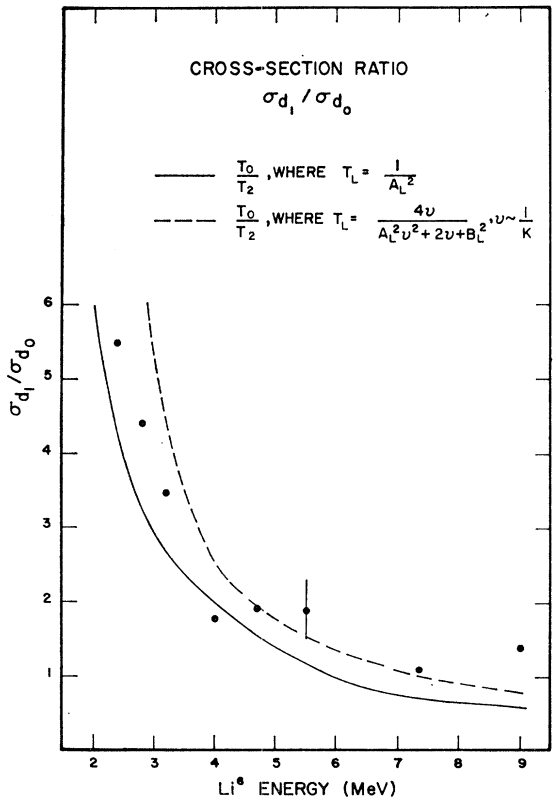

FIG. 27. Ratio of total cross sections of d_1 and d_0. Dashed and solid curves represent transmission coefficient ratios for $L=0$ and $L=2$ calculated with the formulas given in the figure. A_L^2 and B_L^2 are the sums of squares of regular and irregular Coulomb wave functions, respectively.

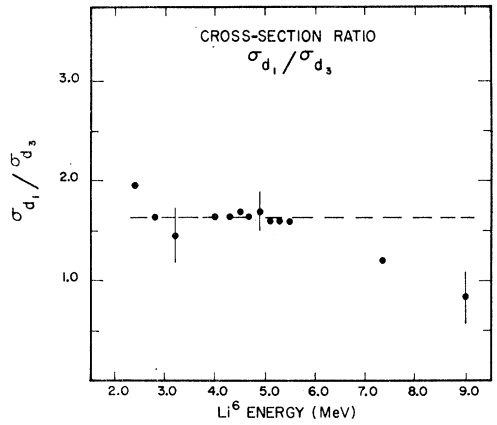

FIG. 28. Ratio of total cross section of d_1 and d_3. Dashed curve is average value of ratio in 4.0–5.5-MeV region.

Because of the larger number of data for the first three observed deuteron groups, the remaining discussion will concern these states primarily. The cross sections for all three are rather rapidly increasing from 2.4 to 4.0 MeV, and slowly increasing above this, with no definite indication of structure. Previous attempts at describing lithium reactions with simple Butler stripping theory have been qualitatively successful (cf. Ref. 30). Since the cluster structure of Li^6 as $(\alpha+d)$ is often quite evident (separation energy is 1.46 MeV), one might instead consider a simple tunneling picture of an α penetrating the total barrier $(\alpha+Li^6)$ to form B^{10} in these three states. The α must carry $l=2$ for ground-state formation and $l=0$ for the first and third excited states.

Figures 27 and 28 show the results of these barrier-penetration considerations. The points are the experimental cross-section ratios and the curves of Fig. 27 represent the ratio of transmission coefficients calculated from Coulomb wave function tables[18] in slightly different ways. The results for $\sigma_{d_1}/\sigma_{d_0}$ are quite encouraging. The ratio $\sigma_{d_1}/\sigma_{d_3}$ (Fig. 28) should be constant as a function of energy if both states are indeed formed by $l=0$ transfer, and the results are again quite good. The greatest deviation from constant ratio occurs at the high-energy end where the experimental statistics are not as good, and also where the barrier-penetration picture might not be as applicable as at lower energies.

These indications of a tunneling mechanism lead one to consider the applicability of the semiclassical Breit-Ebel tunneling theory.[32] An examination of the assumptions involved in this theory is not particularly encouraging for the present case, however. The Coulomb parameter η, which should be much greater than unity, is only about 2.2 at 2.4 MeV, possibly not large enough to justify the use of classical orbits. Although we are below the incoming barrier at the lower energies, the outgoing energies are always greater than the exit-

[32] G. Breit and M. E. Ebel, Phys. Rev. **103**, 679 (1956); **104**, 1030 (1956).

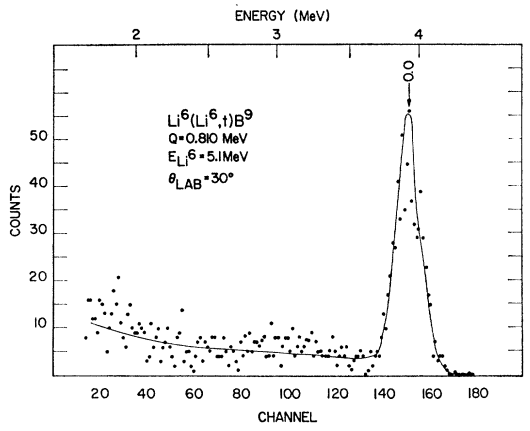

FIG. 29. Energy spectrum of tritons from $Li^6(Li^6,t)B^9$. See caption for Fig. 2.

channel Coulomb barrier. The most troublesome point, however, is that the transferred particle is an α, which has quite sizeable mass and charge with respect to the target and projectile.

The general result of such tunneling considerations is that the yield curves increase more slowly than predicted. This effect is often explained by the presence of virtual Coulomb excitation[32] (VCE), but a quantitative description of this phenomenon is not available for the present case. It might be preferable to refer, at large distances, to a long-range effective interaction (LREI), which tends to raise the cross sections above the simple tunneling magnitude. Qualitatively at least, the shapes of the angular distributions for d_0, d_1, and d_3 are similar to those presented in Ref. 32 for tunneling in the presence of LREI or VCE to various regions of the continuum. Thus although an α-tunneling mechanism is indicated, the simple Breit-Ebel theory does not agree very well with the experimental results unless long-range interaction effects are assumed to be important.

This semiclassical α tunneling has been recently investigated in (N^{14},F^{18}) reactions,[33] but there the projectile is at least much more massive than the transferred particle. One important result of that investigation was the strong dependence of the cross section on the α-particle binding energy of the target nucleus. This is reasonable, since the Breit-Ebel cross sections vary as e^X where X contains the binding energy of the particle being transferred. A comparison of (Li^6,d_0) from the present work with the (Li^6,d_0) reactions[8] on B^{10} and B^{11} (α-separation energies 4.46 and 8.67 MeV, respectively), at bombarding energies corresponding to the same fraction of the Coulomb barrier height, does indeed indicate a rapid decrease of the cross section with increasing α-separation energy. It is, of course, not clear that the reaction mechanism is the same in these experiments, but further evidence for a tunneling mechanism in (Li^6,d) is perhaps indicated.

[33] R. M. Gaedke, K. S. Toth, and I. R. Williams, Phys. Rev. 140, B296 (1965).

Particularly at low energies then, an outstanding mechanism of interaction is via the transfer of an α particle, and this mode is quite favored if a state may be formed by an $l_\alpha=0$ transfer. This mode of interaction seems to be dominant over most of the energy range studied, and the cross sections apparently change with energy as expected from a simple transmission-coefficient calculation.

TRITONS: RESULTS

A typical triton spectrum is shown in Fig. 29. Only one prominent group, t_0 from the B^9 ground state, is evident. A continuum is also seen, probably due to the Be^8+t+p final state possible from $B^9 \rightarrow Be^8+p$. Since the Q is only 810 keV for the B^9+t exit channel, it was quite difficult, even at forward angles, to reach a very high excitation in B^9. In fact the upper limit in observable excitation was only slightly above 2 MeV, which does not include the first excited state at 2.34 MeV. There was no evidence in this experiment for the existence of a state in the 1.4–1.7-MeV excitation region.

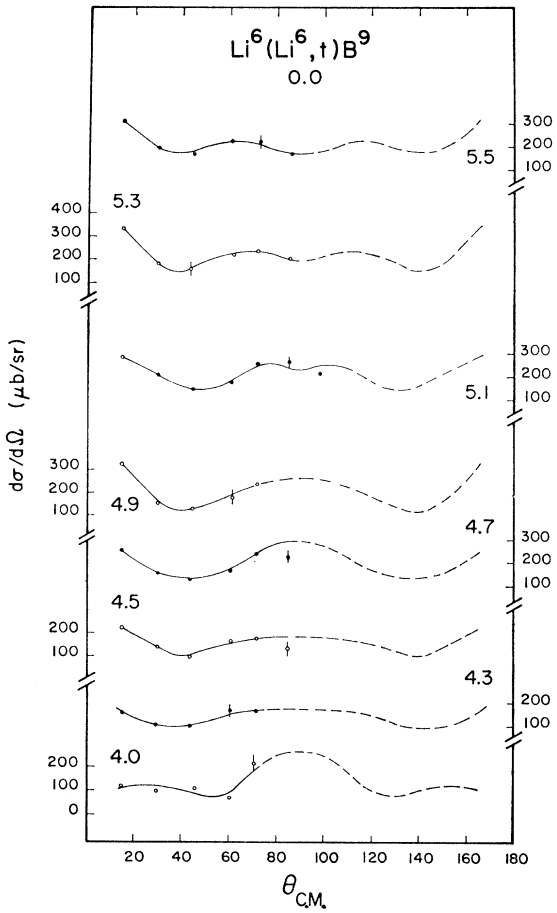

FIG. 30. Angular distributions of tritons from $Li^6(Li^6,t_0)B^9$. Bombarding energy range is 4.0–5.5 MeV. See caption for Fig. 3.

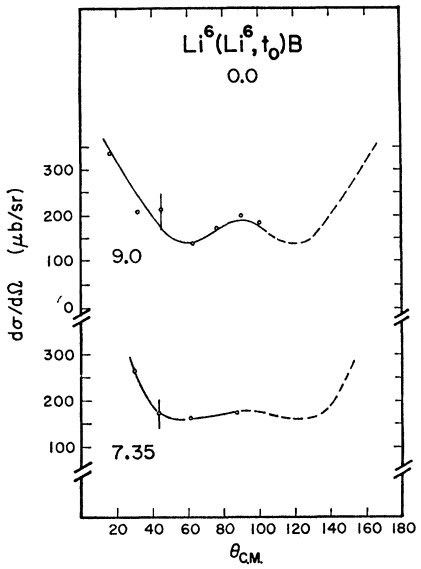

FIG. 31. Angular distributions of tritons from $Li^6(Li^6,t_0)B^9$ at 7.35 and 9.0 MeV. See caption for Fig. 3.

The t_0 angular distributions are shown in Figs. 30 and 31. The shape is fairly constant at all energies, but minor variations are evident. The yield in Fig. 32 increases from 4.0 to 4.7 MeV, and within statistics is constant at higher energies.

It should be pointed out that the errors indicated in the angular distributions represent only statistical errors, as is the case for all other differential cross sections presented here. The total relative error for the tritons is somewhat larger than for other particle groups for two reasons. The first has been mentioned previously, namely the background continuum. This background was subtracted during analysis of the data, and its total contribution to the cross section is estimated to be less than 5%. The second source of error results from the fact that t_0 and d_3 have nearly the same Q (0.81 and 0.84 MeV, respectively). These two groups thus nearly coincide in the E direction in the two-parameter data format at some angles, and because of the great difference in yields (roughly a factor of 5) the deuteron peak sometimes tends to spill over into the triton region in the dE/dx direction.

One point that has not been mentioned is that another energetically possible reaction in this experiment is

$$Li^6+Li^6 \rightarrow Be^9+He^3+1.88 \text{ MeV}.$$

Although it is possible to resolve He^3 and He^4 with our detection system, all charge-2 groups were stored together for convenience in later analysis of the charge-1 data. The possible presence of He^3 in the α results was ruled out by reaction kinematic calculations. Previous work at lower energies has dealt with the comparison of the He^3 and triton results.[14]

TRITONS: DISCUSSION

The angular distributions for t_0 are reasonably constant as a function of incident energy, and the total cross section is fairly smooth within statistics. It is difficult to imagine the reaction as proceeding via the direct process, since this would require transfer of a He^3, and the (He^3+t) separation energy of Li^6 is 15.8 MeV.

In previous work at lower energy,[14] the He^3 and triton results from this reaction were compared on the basis of simple charge-symmetry considerations. The ground-state Q value for production of He^3 is 1.88 MeV, compared with 0.81 MeV for t_0. If one considers the factor-of-two difference in charge, however, the outgoing penetrabilities are nearly the same. The experimental He^3-t cross section ratio agreed well with the ratio of outgoing wave numbers, as expected from charge symmetry, and the angular distributions for He^3 and t were quite similar. These results are consistent with a compound-nucleus mechanism for formation of the B^9 and Be^9 ground states.

The total cross section for formation of the B^9 ground state (typically 2.0–2.5 mb) is quite near the usual proton values, and much lower than the deuteron cross sections. In fact the energy-averaged cross section for t_0 (2.4 mb) is within 20% of that for p_0 (2.0 mb). The spins for both these states are $\frac{3}{2}^-$, if we take this value for B^9 in analogy with the Be^9 ground state. This result fits quite well with a compound-nucleus interpretation for (Li^6,t_0).

ALPHAS: RESULTS

Figure 33 shows a typical α spectrum at 10° (lab). The distinguishing feature is clearly the very prominent peaks which correspond to the 16.62- and 16.92-MeV Be^8 states. A broad continuum at lower excitation is noticeable, but no other structure is apparent. Because experimental gain setting did not permit observation of the low excitation region in Be^8 at most angles, only the 16-MeV region of the alpha spectrum was carefully investigated.

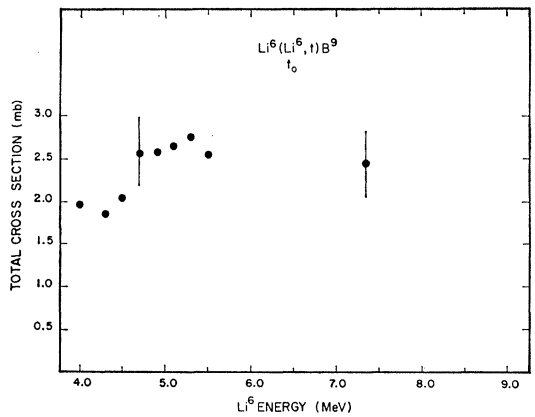

FIG. 32. Total cross sections for t_0. See caption for Fig. 13.

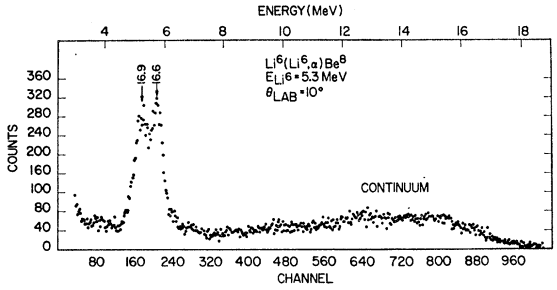

FIG. 33. Energy spectrum of alphas from $Li^6(Li^6,\alpha)Be^8$. See caption for Fig. 2.

Because of the relatively low Q (~4 MeV) to these states, and also because of the amount of foil over the proportional-counter entrance window (typically ~7–8 mg/cm² Al used to stop the scattered beam), the α particles from these states have fairly low energy. At 4.7 MeV, for example, alphas from the 16.6-MeV state have only about 4.1 MeV at 10° lab after the foils, and this is decreased to 3.5 MeV at 20°. Adequate resolution of the states could generally be achieved only at a lab angle of 10°. Because the $dE/d\theta$ is quite large for these groups, even the 20° data were generally not well-enough resolved to be usefully analyzed.

Figure 34 shows an example of the results for the 16-MeV states with greater energy gain. The solid curve is a two-Gaussian least-squares fit to the data. The α peak shape in this region is fortunately obtainable from a thorium α source, which gives an α of nearly the same initial energy (8.78 MeV for the source) as the reaction alphas in this region. A constant background was assumed, and the dashed curves represent the magnitude of this background and the final alpha peaks after background subtraction. The peak-fitting program computes the areas under the peaks and assigns an error to the procedure from considerations of experimental statistics and goodness of fit. Seven fits of this type were obtained at 200-keV intervals between 4.3- and 5.5-MeV incident energy.

One possible source of error in the area under these peaks is the presence of alphas from contaminant reactions, particularly carbon. Small indications of Li^6+C^{12} reactions were sometimes evident in the deuteron spectra, for example. The reaction

$$Li^6+C^{12} \rightarrow N^{14}+\alpha+8.8 \text{ MeV},$$

yields alphas in the energy region of interest. There was no noticeable yield from the N^{14} ground state, but the troublesome groups would be from the next few states, and Heikkinen's results[7] show that these excited-state yields are typically 5–10 times the ground-state yield. Thus although there is apparently no sign of contaminant peaks in the α spectrum, and the shape of the α peaks from Be^8 do not appear distorted at any energies, kinematical calculations indicate such contaminant peaks could interfere in some cases if present.

TABLE I. Yield ratio and differential cross sections for 16.62- and 16.92-MeV states in Be^8.

Li^6 energy (MeV)	Yield ratio (16.6-MeV state)/ (16.9-MeV state)	$d\sigma/d\Omega$ (mb/sr) at 10° lab 16.62 MeV	16.92 MeV
4.3	1.33±0.05	1.4	1.2
4.5	1.09	1.6	1.4
4.7	1.30	2.2	2.1
4.9	1.23	2.3	1.9
5.1	1.05	1.9	1.5
5.3	1.15	2.0	1.9
5.5	1.22	2.2	1.7

Thus the results for the 16-MeV Be^8 states should be taken with these considerations in mind.

Table I contains the computed yield ratios and cross sections for the 16.6- and 16.9-MeV states as a function of incident energy. The error quoted for all ratios, ±0.05, is approximately the maximum error assigned by the fitting routine to any one ratio. The ratio varies somewhat between energies, but no systematic trend is noticeable. A constant mean ratio of 1.20±0.10 is thus assigned. These ratios have previously appeared in another paper from this laboratory.[34] By normalization of the data to the d_0 results at 10°, the absolute differential cross section at this angle was derived for the 16.6-MeV state. Using the yield ratios at each energy, the corresponding values for the 16.9-MeV level were obtained.

ALPHAS: DISCUSSION

It was believed until recently that either the 16.62- or the 16.92-MeV Be^8 state was the $T=1$ analog of the Li^8 and B^8 ground states. Conflicting experimental

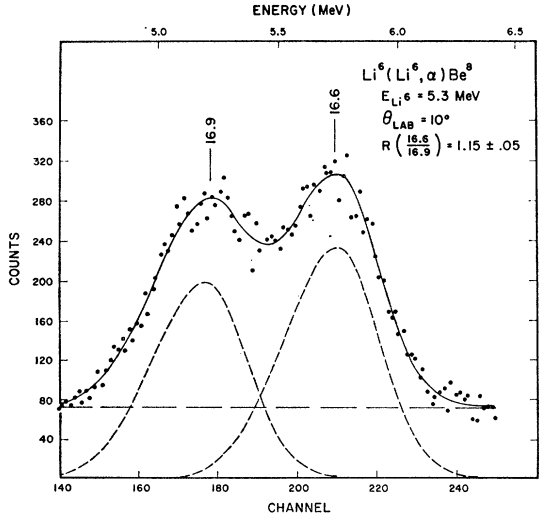

FIG. 34. Energy spectrum of alphas in 16-MeV excitation region from $Li^6(Li^6,\alpha)Be^8$. Solid curve is least-squares fit to data. Dashed line is constant background and dashed curve represents fitted peaks after background subtraction.

[34] M. D. Mancusi and E. Norbeck, Phys. Rev. 151, 830 (1966).

results led Marion to postulate[35] that these are almost pure single-particle states of the following configurations:

$$16.62 \text{ MeV state: } Li^7(\text{g.s.})+p,$$
$$16.92 \text{ MeV state: } Be^7(\text{g.s.})+n.$$

Theoretical calculations (see Ref. 13 for a rather complete review of theory and experiment) indicate that strong isospin mixing of these states is probable. Thus previous experiments (listed in Ref. 13) which indicated a strong isospin violation assuming one of the states had $T=1$ may be explained as proceeding through the $T=0$ components of these states.

The similar yields to these states have been noted at lower energies in this laboratory,[36] and it is now clear that the effect also persists independent of bombarding energy over the 4.3- to 5.5-MeV range. The slightly larger yield of the 16.62-MeV state indicates that the isospin mixing is probably not total.

The cross section for formation of these states is very large, at least at 10° (lab) where the present results were obtained. If one considers the (Li^6,α) process as a deuteron transfer, these 2^+ states could be readily formed by an $l_d=0$ capture. Results from $Li^6(He^3,p)Be^8$ for the 16.6-MeV level indicate $l=0$ stripping with a large deuteron width.[37] The outgoing alphas are undoubtedly quite effective in carrying off the large angular momenta inherent in heavy-ion reactions, which is consistent with the large cross sections in this case.

SUMMARY

The results of the present experiment indicate the presence of competing reaction modes. The relative contribution of each is, however, difficult to assess. It is clear that a favored mechanism of interaction in the (Li^6,d) case is via the transfer of an α, and this mode is even more favored if the transferred cluster needs only $l_\alpha=0$ to form the residual state. Simple considerations of the transfer as a tunneling process possibly modified by the effects of a long-range effective interaction results in an adequate description of the deuteron cross sections.

Comparison of the proton and triton results with mirror exit-channel configurations indicate a compound-nucleus picture is most likely for these emissions. The proton and triton cross sections are considerably smaller than the deuteron ones, and the angular distributions show significant variation as a function of incident energy in many cases. The high excitation energies reached in the C^{12} compound system make the occurrence of a statistical compound nucleus likely, and this appears to be the case for (Li^6,p) as the incident energy increases. The high yields for the 7.30- and 7.99-MeV states in B^{11} are, however, suggestive of a direct 5-nucleon-transfer formation mode, and thus a significant direct contribution to the proton cross sections cannot be ruled out.

The differential-cross-section ratio of the 16.62- and 16.92-MeV states in Be^8 was found to be constant at 1.20 as a function of incident energy. This result is quite reasonable in terms of Marion's description of these states as single-nucleon in character, and thus not of pure isospin.[13]

Quantitative fits of the data were not presented, but such treatments might well be made with some success. At the high energies, one might hope that for (Li^6,d) a DWBA calculation could adequately describe the process. The emphasis here has been on a qualitative understanding of the results, which is a prerequisite before one can attempt to obtain reliable spectroscopic information.

ACKNOWLEDGMENTS

The author is indebted to Professor R. R. Carlson for his advice throughout the course of this work. Discussions with Professor R. T. Carpenter and Dr. R. M. Bahnsen proved quite valuable, and W. A. Seale and M. J. Throop rendered great assistance during long data runs.

[35] J. B. Marion, Phys. Letters **14**, 315 (1965).
[36] R. R. Carlson and K. G. Kibler, University of Iowa Report SUI-64-21, 1964 (unpublished).
[37] F. Morinigo, Nucl. Phys. **50**, 136 (1964).